International Journal of Mathematical Archive-3(6), 2012, 2258-2272
Available online through www.ijma.info ISSN 2229 – 5046

THE EFFECT OF RADIATION AND HALL CURRENTS ON CONVECTIVE HEAT AND MASS TRANSFER FLOW OF A VISCOUS ELECTRICALLY CONDUCTING FLUID IN A VERTICAL WAVY CHANNEL WITH INTERNAL HEAT SOURCES

A. Veera Suneela Rani[1], Dr. V. Sugunamma[1] and Prof. D. R. V. Prasada Rao[2*]

[1]Department of Mathematics, Sri Venkateswara University, Tirupati, Andhrapradesh, India
[2]Professor, Dept. of Mathematics, S. K. University, Anantapur, Andhrapradesh, India

(Received on: 22-05-12; Accepted on: 11-06-12)

ABSTRACT

We investigate the convective study of heat and mass transfer flow of a viscous electrically conducting fluid in a vertical wavy channel under the influence of an inclined magnetic fluid with heat generating sources. The walls of the channels are maintained at constant temperature and concentration. The equations governing the flow heat and concentration are solved by employing perturbation technique with a slope δ of the wavy wall. The velocity, temperature and concentration distributions are investigated for a different values of D^{-1} M, m, N, N1, α . The rate of heat and mass transfer are numerically evaluated for a different variations of the governing parameters

Key words: *Radiation effect, Hall currents, Heat and mass transfer, Wavychannel, Heat sources.*

1. INTRODUCTION

The flow of heat and mass from a wall embedded in a porous media is a subject of great interest in the research activity due to its practical applications; the geothermal processes, the petroleum industry, the spreading of pollutants, cavity wall insulations systems, flat-plate solar collectors, flat-plate condensers in refrigerators, grain storage containers, nuclear waste management.

The flow takes place both axially (primary) and transversely (secondary) with the secondary velocity being towards the axis in the fluid bulk rather than confining within a thin layer as in straight channels. Hence it is advantageous to go for converging-diverging geometries for improving the design of heat transfer equipment. Later Vajravelu and Debnath [16] have extended this study to convective flow is a vertical wavy channel in four different geometrical configurations. This problem has been extended to the case of wavy walls by, Deshikachar et al [5] Rao *et. al.*, [11] and Sree Ramachandra Murthy [15]. Mahdy *et. al.*, [8] have studied the mixed convection heat and mass transfer on a vertical wavy plate embedded in a saturated porous media (PST/PSE) Comini *et. al.*, [4] have analyzed the convective heat and mass transfer in wavy finned-tube exchangers.

Rajesh et al [12] have discussed the time dependent thermal convection of a viscous, electrically conducting fluid through a porous medium in horizontal channel bounded by wavy walls. Kumar [12] has discussed the two-dimensional heat transfer of a free convective MHD (Magneto Hydro Dynamics) flow with radiation and temperature dependent heat source of a viscous incompressible fluid, in a vertical wavy channel. Recently Mahdy et al [8] have presented the Non-similarity solutions have been presented for the natural convection from a vertical wavy plate embedded in a saturated porous medium in the presence of surface mass transfer.

In all these investigations, the effects of Hall currents are not considered. However, in a partially ionized gas, there occurs a Hall current when the strength of the impressed magnetic field is very strong. These Hall effects play a significant role in determining the flow features. Yamanishi [17] have discussed the Hall effects on the steady hydromagnetic flow between two parallel plates. Alam *et. al.*,[2] have studied unsteady free convective heat and mass transfer flow in a rotating system with Hall currents, viscous dissipation and Joule heating. Taking Hall effects in to account Krishna *et. al.*, [7] have investigated Hall effects on the unsteady hydromagnetic boundary layer flow. Rao *et. al.*, [11] have analyzed Hall effects on unsteady Hydromagnetic flow. Siva Prasad *et. al.*, [14] have studied Hall effects on unsteady MHD free and forced convection flow in a porous rotating channel. Anwar Beg et al(3) have discussed unsteady magnetohydrodynamics Hartmann-Couette flow and heat transfer in a Darcian channel with Hall current,ionslip, Viscous and Joule heating effects .Ahmed [1] has discussed the Hall effects on transient flow pas an

****Corresponding author:** Prof. D. R. V. Prasada Rao[2*]*
[2]Professor, Dept. of Mathematics, S. K. University, Anantapur, Andhrapradesh, India

impulsively started infinite horizontal porous plate in a rotating system. Shanti [13] has investigated effect of Hall current on mixed convective heat and mass transfer flow in a vertical wavy channel with heat sources. Leela [9] has studied the effect of Hall currents on the convective heat and mass transfer flow in a horizontal wavy channel under inclined magnetic field.

In this paper we investigate the convective study of heat and mass transfer flow of a viscous electrically conducting fluid in a vertical wavy channel under the influence of an inclined magnetic fluid with heat generating sources. The walls of the channels are maintained at constant temperature and concentration. The equations governing the flow heat and concentration are solved by employing perturbation technique with a slope δ of the wavy wall. The velocity, temperature and concentration distributions are investigated for a different values of D^{-1} M, m, N, N_1,α . The rate of heat and mass transfer are numerically evaluated for a different variations of the governing parameters.

2. FORMULATION AND SOLUTION OF THE PROBLEM

We consider the steady flow of an incompressible, viscous ,electrically conducting fluid confined in a vertical channel bounded by two wavy walls under the influence of an inclined magnetic field of intensity Ho lying in the plane (y-z).The magnetic field is inclined at an angle $\alpha 1$ to the axial direction k and hence its components are $(0, H_0 Sin(\alpha_1), H_0 Cos(\alpha_1))$ .In view of the waviness of the wall the velocity field has components(u,0,w)The magnetic field in the presence of fluid flow induces the current($(J_x, 0, J_z)$ .We choose a rectangular cartesian co-ordinate system O(x, y, z) with z-axis in the vertical direction and the walls at $x = \pm f(\frac{\delta z}{L})$.

The Momentum equations including Hall currents are

$$u\frac{\partial u}{\partial x} + w\frac{\partial u}{\partial z} = -\frac{\partial p}{\partial x} + \mu\left(\frac{\partial^2 u}{\partial x^2} + \frac{\partial^2 u}{\partial z^2}\right) - \frac{\sigma\mu_e H_{00}^2 Sin^2(\alpha_1)}{1 + m^2 H_0^2 Sin^2(\alpha_1)}(u + mH_0 wSin(\alpha_1)) - \left(\frac{\mu}{k}\right)u \tag{1}$$

$$u\frac{\partial W}{\partial x} + w\frac{\partial W}{\partial z} = -\frac{\partial p}{\partial z} + \mu\left(\frac{\partial^2 W}{\partial x^2} + \frac{\partial^2 W}{\partial z^2}\right) - \frac{\sigma\mu_e H_0^2 Sin^2(\alpha_1)}{1 + m^2 H_0^2 Sin^2(\alpha_1)}(w - mH_0 uSin(\alpha_1)) - \left(\frac{\mu}{k}\right)W - \rho g \tag{2}$$

The energy equation is

$$\rho C_p (u\frac{\partial T}{\partial x} + w\frac{\partial T}{\partial z} = k_f (\frac{\partial^2 T}{\partial x^2} + \frac{\partial^2 T}{\partial z^2}) + Q(T_e - T) - \frac{\partial (q_r)}{\partial x} \tag{3}$$

The diffusion equation is

$$(u\frac{\partial C}{\partial x} + w\frac{\partial C}{\partial z} = D_1 (\frac{\partial^2 C}{\partial x^2} + \frac{\partial^2 C}{\partial z^2}) + k_{11} (\frac{\partial^2 T}{\partial x^2} + \frac{\partial^2 T}{\partial z^2}) \tag{4}$$

The equation of state is

$$\rho - \rho_0 = -\beta(T - T_o) - \beta^{\bullet}(C - C_o) \tag{5}$$

Where T,C are the temperature and concentration in the fluid. k_f is the thermal conductivity, Cp is the specific heat constant pressure,D_1 is molecular diffusivity,k_{11} is the cross diffusivity, β is the coefficient of thermal expansion, $\beta^{\bullet}$ is the coefficient of volume expansion ,Q is the strength of the heat source and q_r is the radiative heat flux.

By Rosseland approximation (Brewester [3a]) the radiative heat flux is given by

$$q_r = -\frac{4\sigma^{\bullet}}{3\beta_r}\frac{\partial (T'^4)}{\partial y} \tag{6}$$

Expanding T'^4 about Te by Taylor expansion and neglecting the higher order terms we get

$$T'^4 \cong 4TT_e^3 - 3T_e^4 \tag{7}$$

Where $\sigma^{\bullet}$ is the Stefan-Boltzman constant and β_r is the mean absorption coefficient. Substituting (6) & (7) in (3) we obtain (8)

The flow is maintained by a constant volume flux for which a characteristic velocity is defined as

$$q = \frac{1}{L}\int_{-Lf}^{Lf} w dx \tag{9}$$

The boundary conditions are

u= 0, w=0 T=T1, C=C_1 on $x = -f(\frac{\delta z}{L})$ (10)

w=0, w=0, T=T_2 ,C=C_2 on $x = f(\frac{\delta z}{L})$ (11)

Eliminating the pressure from equations(1)&(2) and introducing the Stokes Stream function ψ as

$$u = -\frac{\partial \psi}{\partial z} \quad , \; w = \frac{\partial \psi}{\partial x} \tag{12}$$

the equations (2.8) & (2.9), (2.15) & (2.11) in terms of ψ is

$$\frac{\partial \psi}{\partial z}\frac{\partial(\nabla^2\psi)}{\partial x} - \frac{\partial \psi}{\partial x}\frac{\partial(\nabla^2\psi)}{\partial z} = \mu\nabla^4\psi + \beta g\frac{\partial(T-T_e)}{\partial x}\beta^{\bullet} g\frac{\partial(C-C_e)}{\partial x} - \left(\frac{\sigma\mu_e^2 H_0^2 Sin^2(\alpha_1)}{1+m^2H_0^2\,Sin^2(\alpha_1)} + \frac{\mu}{k}\right)\nabla^2\psi \tag{13}$$

$$\rho C_p\left(\frac{\partial \psi}{\partial x}\frac{\partial T}{\partial z} - \frac{\partial \psi}{\partial z}\frac{\partial T}{\partial x} = k_f\left(\frac{\partial^2 T}{\partial x^2} + \frac{\partial^2 T}{\partial z^2}\right) + Q(T_e - T) + \frac{16\sigma^{\bullet}T_e^3}{3\beta_R}\frac{\partial^2 T}{\partial x^2}\right. \tag{14}$$

$$\left(\frac{\partial \psi}{\partial x}\frac{\partial C}{\partial z} - \frac{\partial \psi}{\partial z}\frac{\partial C}{\partial x} = D_1\left(\frac{\partial^2 C}{\partial x^2} + \frac{\partial^2 C}{\partial z^2}\right) + k_{11}\left(\frac{\partial^2 C}{\partial x^2} + \frac{\partial^2 C}{\partial z^2}\right)\right. \tag{15}$$

On introducing the following non-dimensional variables

$$(x', z') = (x, z)/L\,, \psi' = \frac{\psi}{qL},\; \theta = \frac{T - T_2}{T_1 - T_2}, C' = \frac{C - C_2}{C_1 - C_2}$$

the equation of momentum and energy in the non-dimensional form are

$$\nabla^4\psi - M_1^2\nabla^2\psi + \frac{G}{R}\left(\frac{\partial\theta}{\partial x} + N\frac{\partial C}{\partial x}\right) = R\left(\frac{\partial \psi}{\partial z}\frac{\partial(\nabla^2\psi)}{\partial x} - \frac{\partial \psi}{\partial x}\frac{\partial(\nabla^2\psi)}{\partial z}\right) \tag{16}$$

$$PR\left(\frac{\partial \psi}{\partial x}\frac{\partial \theta}{\partial z} - \frac{\partial \psi}{\partial z}\frac{\partial \theta}{\partial x}\right) = \nabla^2\theta - \alpha\,\theta + \frac{4}{3N_1}\frac{\partial^2\theta}{\partial x^2} \tag{17}$$

$$ScR\left(\frac{\partial \psi}{\partial x}\frac{\partial C}{\partial z} - \frac{\partial \psi}{\partial z}\frac{\partial C}{\partial x}\right) = \nabla^2 C + \frac{ScSo}{N}\nabla^2\theta \tag{18}$$

where

$G = \frac{\beta g\,\Delta T_e L^3}{\nu^2}$ (Grashof Number), $M^2 = \frac{\sigma\mu_e^2 H_o^2 L^2}{\nu^2}$ (Hartman Number)

$M_1^2 = \frac{M^2 Sin^2(\alpha_1)}{1+m^2}$, $R = \frac{qL}{\nu}$ (Reynolds Number)

$P = \frac{\mu C_p}{K_f}$ (Prandtl Number), $\alpha = \frac{QL^2}{\Delta T K_f}$ (Heat Source Parameter)

$Sc = \frac{\nu}{D_1}$ (Schmidt Number), $S_o = \frac{k_{11}\beta^\bullet}{\nu\beta}$ (Soret parameter)

$N = \frac{\beta^*(C_1 - C_2)}{\beta(T_1 - T_2)}$ (Buoyancy ratio), $N_1 = \frac{3\beta_R K_f}{4\sigma^\bullet T_e^3}$ (Radiation parameter)

The corresponding boundary conditions are

$$\psi(f) - \psi(-f) = 1$$

$$\frac{\partial\psi}{\partial z} = 0, \frac{\partial\psi}{\partial x} = 0, \theta = 1, C = 1 \quad at\ x = -f(\delta z)$$

$$\frac{\partial\psi}{\partial z} = 0, \frac{\partial\psi}{\partial x} = 0, \theta = 0\ , C = 0 \quad at\ x = +f(\delta z)$$

3. ANALYSIS OF THE FLOW

Introduce the transformation such that

$$\bar{z} = \delta z, \frac{\partial}{\partial z} = \delta \frac{\partial}{\partial \bar{z}}$$

Then

$$\frac{\partial}{\partial z} \approx O(\delta) \rightarrow \frac{\partial}{\partial \bar{z}} \approx O(1)$$

For small values of δ <<1,the flow develops slowly with axial gradient of order δ and hence we take $\frac{\partial}{\partial \bar{z}} \approx O(1).$

Using the above transformation the equations (2.23)-(2.25) reduce to

$$F^4\psi - M_1^2 F^2\psi + \frac{G}{R}\left(\frac{\partial\theta}{\partial x} + N\frac{\partial C}{\partial x}\right) = \delta R\left(\frac{\partial\psi}{\partial\bar{z}}\frac{\partial(F^2\psi)}{\partial x} - \frac{\partial\psi}{\partial x}\frac{\partial(F^2\psi)}{\partial\bar{z}}\right) \tag{19}$$

$$\delta P_1 R\left(\frac{\partial\psi}{\partial x}\frac{\partial\theta}{\partial z} - \frac{\partial\psi}{\partial z}\frac{\partial\theta}{\partial x}\right) = F^2\theta - \alpha_2\theta \tag{20}$$

$$\delta ScR\left(\frac{\partial\psi}{\partial x}\frac{\partial c}{\partial z} - \frac{\partial\psi}{\partial z}\frac{\partial C}{\partial x}\right) = F^2 C + \frac{ScSo}{N}F^2\theta \tag{21}$$

where

$$F^2 = \frac{\partial}{\partial x^2} + \delta^2\frac{\partial}{\partial\bar{z}^2}$$

$$P_1 = \frac{3N_1 P}{3N_1 + 4}\ ,\ \alpha_2 = \frac{3N_1\alpha}{3N_1 + 4}$$

Assuming the slope δ of the wavy boundary to be small we take

$$\psi(x,z) = \psi_0(x,y) + \delta\psi_1(x,z) + \delta^2\psi_2(x,z) + \ldots\ldots\ldots\ldots$$
$$\theta(x,z) = \theta_o(x,z) + \delta\theta_1(x,z) + \delta^2\theta_2(x,z) + \ldots\ldots\ldots\ldots \quad (22)$$
$$C(x,z) = C_o(x,z) + \delta c_1(x,z) + \delta^2 c_2(x,z) + \ldots\ldots\ldots\ldots$$

Let $\eta = \dfrac{x}{f(\bar{z})}$ (23)

Substituting (3.3) in equations (19)&(20) and using (22) and equating the like powers of δ the equations and the respective boundary conditions to the zeroth order are

$$\frac{\partial^2\theta_0}{\partial\eta^2} - (\alpha_2 f^2)\theta_0 = 0 \quad (24)$$

$$\frac{\partial^2 C_0}{\partial\eta^2} = -\frac{\mathrm{Sc\,So}}{\mathrm{N}}\frac{\partial^2\theta_0}{\partial\eta^2} \quad (25)$$

$$\frac{\partial^4\psi_0}{\partial\eta^4} - (M_1^2 f^2)\frac{\partial^2\psi_0}{\partial\eta^2} = -\frac{Gf^3}{R}\left(\frac{\partial\theta_0}{\partial\eta} + N\frac{\partial C_0}{\partial\eta}\right) \quad (26)$$

with

$$\psi_0(+1) - \psi_0(-1) = 1$$
$$\frac{\partial\psi_0}{\partial\eta} = 0,\ \frac{\partial\psi_0}{\partial\bar{z}} = 0, \quad \theta_0 = 1\ ,\ C_0 = 1 \quad at \quad \eta = -1 \quad (27)$$
$$\frac{\partial\psi_0}{\partial\eta} = 0,\ \frac{\partial\psi_0}{\partial\bar{z}} = 0, \quad \theta_0 = 0\ ,\ C_0 = 0 \quad at \quad \eta = +1$$

and to the first order are

$$\frac{\partial^2\theta_1}{\partial\eta^2} - (\alpha_2 f^2)\theta_1 = P_1 Rf\left(\frac{\partial\psi_0}{\partial\eta}\frac{\partial\theta_0}{\partial\bar{z}} - \frac{\partial\psi_0}{\partial\bar{z}}\frac{\partial\theta_0}{\partial\eta}\right) \quad (28)$$

$$\frac{\partial^2 C_1}{\partial\eta^2} = ScRf\left(\frac{\partial\psi_0}{\partial\eta}\frac{\partial C_0}{\partial\bar{z}} - \frac{\partial\psi_0}{\partial\bar{z}}\frac{\partial C_0}{\partial\eta}\right) - \frac{Sc\,So}{N}\frac{\partial^2\theta_1}{\partial\eta^2} \quad (29)$$

$$\frac{\partial^4\psi_1}{\partial\eta^4} - (M_1^2 f^2)\frac{\partial^2\psi_1}{\partial\eta^2} = -\frac{Gf^3}{R}\left(\frac{\partial\theta_1}{\partial\eta} + N\frac{\partial C_1}{\partial\eta}\right) + Rf\left(\frac{\partial\psi_0}{\partial\eta}\frac{\partial^3\psi_0}{\partial z^3} - \frac{\partial\psi_0}{\partial\bar{z}}\frac{\partial^3\psi_0}{\partial x\partial z^2}\right) \quad (30)$$

With

$$\psi_1(+1) - \psi_1(-1) = 0$$
$$\frac{\partial\psi_1}{\partial\eta} = 0,\ \frac{\partial\psi_1}{\partial\bar{z}} = 0, \quad \theta_1 = 0, C_1 = 0 \quad at \quad \eta = -1 \quad (31)$$
$$\frac{\partial\psi_1}{\partial\eta} = 0,\ \frac{\partial\psi_1}{\partial\bar{z}} = 0, \quad \theta_1 = 0\ .C_1 = 0 \quad at \quad \eta = +1$$

The equations (25)-(30) are solved subject to the condition (27) & (31) For the sake brevity the solutions are not presented.

5. NUSSELT NUMBER and SHERWOOD NUMBER

The rate of heat transfer (Nusselt Number) on the walls has been calculated using the formula

$$Nu = \frac{1}{f(\theta_m - \theta_w)}\left(\frac{\partial \theta}{\partial \eta}\right)_{\eta=\pm 1}$$

where

$$\theta_m = 0.5\int_{-1}^{1} \theta \, d\eta$$

$$(Nu)_{\eta=+1} = \frac{1}{f\theta_m}(a_{78} + \delta(a_{76} + a_{77})))$$

$$(Nu)_{\eta=-1} = \frac{1}{f(\theta_m - 1)}(a_{79} + \delta(a_{77} - a_{76})))$$

$$\theta_m = a_{80} + \delta a_{81}$$

The rate of mass transfer (Sherwood Number) on the walls has been calculated using the formula

$$Sh = \frac{1}{f(C_m - C_w)}\left(\frac{\partial C}{\partial \eta}\right)_{\eta=\pm 1}$$

where

$$C_m = 0.5\int_{-1}^{1} C \, d\eta$$

$$(Sh)_{\eta=+1} = \frac{1}{fC_m}(a_{74} + \delta a_{70})$$

$$(Sh)_{\eta=-1} = \frac{1}{f(C_m - 1)}(a_{75} + \delta a_{71})$$

$$C_m = a_{73} + \delta a_{72}$$

5. RESULTS AND DISCUSSION OF THE NUMERICAL RESULTS

In this analysis, we investigate the effect of Hall Currents and wall waviness on convective Heat and Mass transfer flow of a viscous electrically conducting fluid through a porous medium in a vertical wavy channel under the influence of an inclined magnetic field. The variation of v with D^{-1} and M shows that lesser the permeability of the porous mediums higher the Lorentz force smaller |v| in the entire flow region. The region of the reversal flow shrinks in its size with increase in D^{-1} or M, while it enlargers with Hall parameter m. Also |v| enhances with m (fig.5). Fig.6 represents the variation of v with heat source parameter α.It is found that the reversal flow which appears in the right half at $\alpha = 2$ spreads to the entire flow region for $\alpha \geq 6$, while for $\alpha < 0$, the reversal flow zone reduces in its size with increase in $|\alpha| \leq 4$ and disappears with higher $|\alpha| \geq 6$. The magnitude of v experiences an enhancement with increase in $|\alpha|$. The variation of v with Schmidt number Sc shows that lesser the molecular diffusivity larger |v| in the flow region. When the molecular buoyancy force dominates over the thermal buoyancy force the velocity v enhances in magnitude when the buoyancy forces act in the same direction and for the forces acting in opposite directions v enhances in the left half and reduces in the right half (fig. 7). From fig.8, we find that higher the dilation of channel walls lesser |v| in the flow region. Moving along the axial direction the axial velocity enhances in magnitude with increase in $x \leq \pi$ and reduces with $x \geq 2\pi$.

The secondary velocity (u) is shown in figs 1-4 for different parametric values. The variation of u with D^{-1} and M shows that lesser the permeability of the porous medium larger u in the flow region. Also higher the Lorentz force larger u and for further higher Lorentz force smaller u in the flow region. The secondary velocity enhances with increase in $m \leq 1.5$ and reduces with $m \geq 2.5$(fig.1). From fig.2, we find that u enhances with $\alpha > 0$ and reduces with $\alpha < 0$. The variation of u with Sc shows that lesser the molecular diffusivity smaller u and for further lowering of the diffusivity larger u in the flow region. The magnitude of u enhances with $N > 0$ and reduces with increase in |N|(Fig-3). From fig.4, we notice that higher the dilation of the channel walls smaller u and for further higher dilation ($\beta \geq 0.7$) larger u in the entire flow region.

The non-dimensional temperature (θ) is shown in figures 9-12 for different values of D^{-1}, M, m, Sc, N,α, β. We follow the convention that the non-dimensional temperature is positive or negative according as the actual temperature is greater/lesser than T_1. The variation of θ with D^{-1} and M shows that the lesser the permeability for the porous medium / higher the Lorentz force larger the actual temperature in the flow region. Also an increase in the Hall parameter m enhances the actual concentration except in the vicinity of the left boundary η = -1 (fig.9). The variation of θ with Schmidt number Sc shows that the lesser molecular diffusivity larger the actual temperature and for further lowering of the diffusivity smaller the temperature(fig.10). The variation of θ with buoyancy ratio N shows that when the molecular buoyancy force dominates over the thermal buoyancy force the actual temperature reduces when the buoyancy forces act in the same direction and for the forces act in the opposite directions larger temperature in the flow region(fig.10). The variation of θ with heat source parameter α reveals that the actual temperature depreciates with $\alpha>0$ and enhances with $|\alpha|$ (fig.11). The influence of the wall waviness on θ is shown in fig.12. It is found that the higher the dilation of channel walls lesser the actual temperature in the flow region.

The non-dimensional concentration (C) is shown in figs 13-16 for different parametric values. The variation of C with D^{-1} and M shows that lesser the permeability of the porous medium/higher the Lorentz force larger the actual concentration in left half and smaller in the right half. An increase in the Hall parameter m$\leq$1.5 enhances the actual concentration in the left half and reduce sin the right half and higher m$\geq$2.5 smaller in the concentration in the left half and larger in the right half of the channel(fig-13). The variation of C with Sc shows that lesser the molecular diffusivity larger the actual concentration in the left half and lesser in the right half and for further lowering of the diffusivity smaller the concentration in left half and larger in the right half and for still lowering of the diffusivity larger the concentration in the left half and smaller in the right half. When the molecular buoyancy force dominates over the thermal buoyancy force the actual concentration enhances in the left half and reduces in the right half, when the molecular buoyancy forces act in the same direction and for the forces acting in opposite direction the actual concentration reduces in the left half and enhances in the right half (fig.14). From fig. 15, we notice that the actual concentration depreciates in the left half and enhances in the right half. In the case of heat sink, the actual concentration enhances in the left half and reduces in the right half with $|\alpha| \leq 4$, while $||\alpha|\geq 6$ it reduces marginally in the entire flow region. The influence of wall waviness on C is shown in fig.26. It is found that higher the dilation of the channel walls lesser the concentration in the left half and larger in the right half and for further higher dilation larger the concentration in the left half and lesser in the right half.

The average Nusselt number (Nu) at $\eta = \pm 1$ is shown in tables 1-8 for different values of G, D^{-1}, M, m, Sc, λ, α, N, β, R. It is found that the rate of heat transfer enhances with increase in G>0 and reduces with G<0 at both the walls. The variation of Nu with D^{-1} shows that lesser the permeability of the porous medium smaller |Nu| at η = +1 and at η = -1, smaller |Nu| and for further lowering of the permeability it depreciates for G<0 and enhances for G>0. The variation of Nu with Hartman number M shows that the higher the Lorentz force lesser |Nu| at η=+1, larger |Nu| for G>0 and smaller |Nu| for G<0. An increase in the Hall parameter m enhances Nu at η = +1 and reduces at η = -1 (tables 1 and 5). The variation of Nu with Schmidt number Sc shows that lesser the molecular diffusivity larger |Nu| at η = +1 and smaller |Nu| at η = -1 in the heating case while in the cooling case larger |Nu| at $\eta = \pm 1$. An increase in the inclination of the magnetic field reduces Nu at η = +1 and enhances it at η = -1 for G>0 while for G<0 a reversed effect is noticed in the behaviour of Nu (tables 2 and 6). The variation of Nu with heat source parameter α shows that the rate of heat transfer reduces at η = +1 and enhances at η = -1. with increase in the strength of the heat source, while in the case of heat sink Nu reduces at η = +1 and at η = -1 it enhances with $|\alpha| \leq 4$ and reduces with $|\alpha|\geq 6$. When the molecular buoyancy force dominates over the thermal buoyancy force, the rate of heat transfer enhances at η = +1 for all G and at η = -1, it enhances in the heating case, depreciates in the cooling case, when the buoyancy forces act in the same directions and for the forces acting in opposite directions the rate of heat transfer reduces for G>0 and enhance for G<0 at both the walls (tables 3 and 7).

The rate of Mass transfer (Sh) at $\eta = \pm 1$ is shown in tables 9-16. It is found that the rate of mass transfer depreciates at η = +1 and enhances at η = -1 with increase in G>0, while for G<0, |Sh| enhances at η = +1 and reduces at η = -1. The variation of Sh with Darcy parameter D^{-1} shows that lesser the permeability of the porous media smaller |Sh| for G>0 and larger for G<0 at both the walls. Higher the Lorentz force smaller Sh at η = +1. An increase in the Hall parameter m enhances |Sh| at $\eta = \pm 1$ for G>0 while for G<0 it reduces at η = +1 and enhances at η = -1. (tables 9 and 13). The variation of Sh with the Schmidt number Sc shows that lesser the molecular diffusivity larger |Sh| at η = +1 and enhances at η = -1(tables 10 and 14). The variation of Sh with heat source parameter α indicates that an increase in the strength of the heat source enhances Sh at η = +1 and enhances at η = -1. A reversed effect is observed in behaviour of |Sh| with increase in the strength of heat sink. The variation of Sh with buoyancy ratio N shows that the rate of mass transfer enhances for G>0 and reduces G<0 when the buoyancy forces act in the same direction and for the forces acting in the opposite directions |Sh| reduces at $\eta = \pm 1$ for G>0 and for G<0 it reduces at η = +1 and enhances at η = -1 (tables 11 and 15). The influence of the surface geometry on Sh is shown in tables 12 and 16. It is found that at η = +1, higher the dilation of the channel walls larger Sh and for further higher dilation smaller Sh for G>0 and smaller |Sh| for

G<0 and at $\eta = -1$ smaller Sh for all G. An increase in the Reynolds number R results in an enhancement in |Sh| at $\eta = \pm 1$.

7. REFERENCES

[1] Ahmed N and H.K. Sarmah: MHD Transient flow past an impulsively started infinite horizontal porous plate in a rotating system with hall current: Int J. of Appl. Math and Mech. 7(2) : 1-15, 2011.

[2] Alam, M.M and Sattar, M.A: Unsteady free convection and mass transfer flow in a rotating system with Hall currents,viscous dissipation and Joule heating ., Joural of Energy heat and mass transfer,V.22,pp.31-39(2000)

[3] Anwar Beg, O, Joaquin Zueco and Takhar, H.S: Unsteady magneto-hydrodynamic Hartmann-Couette flow and heat transfer in a Darcian channel with hall currents, ionslip, Viscous and Joule heating: Network Numerical solutions, Commun Nonlinear Sci Numer Simulat,V.14,pp.1082-1097(2009).

[4] Comini.G,C. Nomino and S. Savino: Convective heat and mass transfer in wavy finned-tube exchangers., Int. J. Num. Methods for heat and fluid flow.,V.12(6), pp.735-755(2002)

[5] Deshikachar,K.S and Ramachandra Rao,A: Effect of a magnetic field on the flow and blood oxygenation in channel of variables cross section , Int.J.Engg.Sci,V.23, p.1121(1985)

[6] Hyon Gook Wan,Sang Dong Hwang,Hyung He Cho:flow and heat /mass transfer in a wavy duct with various corrugation angles in two-dimensional flow.Heat and Mass transfer ,V.45,pp.157-165(2008)

[7] Krishna, D.V,Prasadarao, D.R.V, Ramachandra urty, A.S: Hydromagnetic convection flow through a porous medium in a rotating channel., J. Engg. Phy. and Thermo. Phy, V.75(2), pp.281-291(2002)

[8] Mahdy A, Mohamed R.A, and Hady F.M.: Natural Convection Heat and Mass Transfer over a vertical wavy surface with variable wall temperature and concentration in porous media: Int. J. of Appl. Math and Mech. 7(3): 1-13,2011.

[9] Naga Leela Kumari: Effect of Hall current on the convective heat and mass transfer flow of a viscous fluid in a horizontal channel, Pesented at APSMS conference, SBIT, Khammam, 2011

[10] Rajesh Yadav Y , Rama Krishna S and Reddaiah P : Mixed Convective Heat transfer through a porous medium in a Horizontal wavy channel. Int. J. of Appl. Math and Mech. 6(17): 25-54, 2010.

[11] Rao,D.R.V,Krishna, D.V and Debnath, L: Combined effect of free and forced convection on Mhd flow in a rotating porous channel, Int. J. Maths and Math.Sci,V.5, pp.165-182(1982)

[12] Rathish Kumar B.V., Shalini Gupta. : Combined influence of mass and thermal stratification on double diffusion non-Darcian natural convection form a wavy vertical channel to porous media, ASME J. Heat Transfer 127(2005) 637-647.

[13] Shanti G: Hall effects on convective heat and mass transfer flow of a viscous fluid in a vertical wavy channel with oscillatory flux and radiation, J. Phys and Appl.Phya, V.22, n0.4, 2010

[14] Sivaprasad, R, Prasada Rao, D.R.V and Krishna, D.V: Hall effects on unsteady Mhd free and forced convection flow in a porous rotating channel., Ind.J. Pure and Appl.Maths, V.19 (2) pp.688-696(1988)

[15] Sreeramachandra Murthy, A: Buoyancy induced hydromagnetic flows through a porous medium-A study ,Ph.D thesis, S.K.University, Anantapur, A.P, India (1992)

[16] Vajravelu, K and Debnath, L: Non-linear study of convective heat transfer and fluid flows induced by traveling thermal waves,Acta Mech,V.59, pp.233-249(1986)

[17] Yamanishi, T:Hall effects on hydromagnetic flow between two parallel plates., Phy. Soc., Japan, Osaka, V.5,p.29 (1962)

Figures:

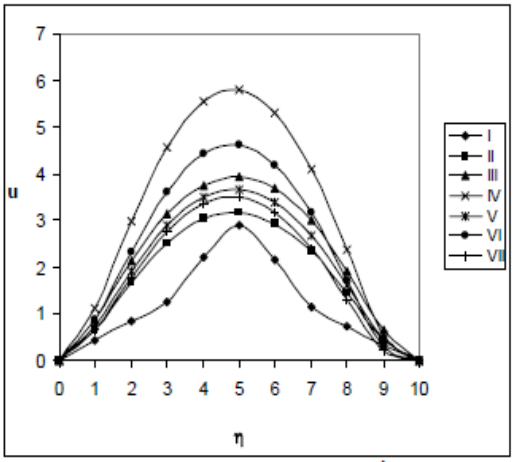

Fig1 : Variation of u with D^{-1}, M, m

	I	II	III	IV	V	VI	VII
D^{-1}	10^2	$2x10^2$	$3x10^2$	10^2	10^2	10^2	10^2
M	2	2	2	4	6	2	2
m	0.5	0.5	0.5	0.5	0.5	1.5	2.5

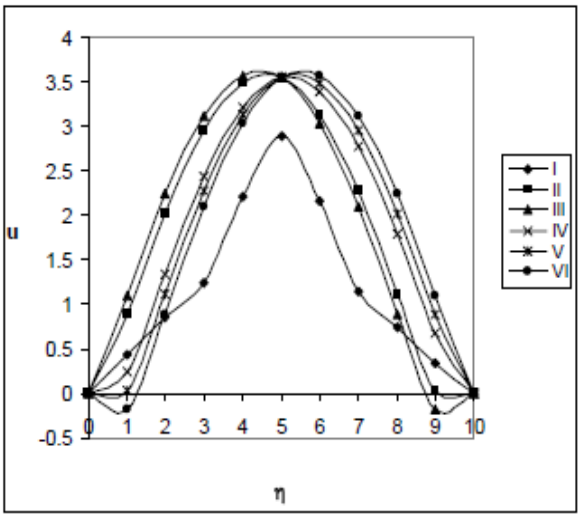

Fig. 2 : Variation of u with α

	I	II	III	IV	V	VI
α	2	4	6	-2	-4	-6

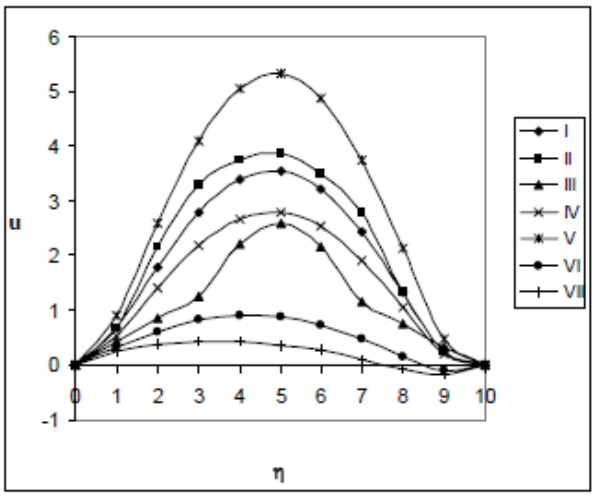

Fig. 3 : Variation of u with Sc, N

	I	II	III	IV	V	VI	VII
Sc	0.24	0.6	1.3	2.01	1.3	1.3	1.3
N	1	1	1	1	2	-0.5	-0.8

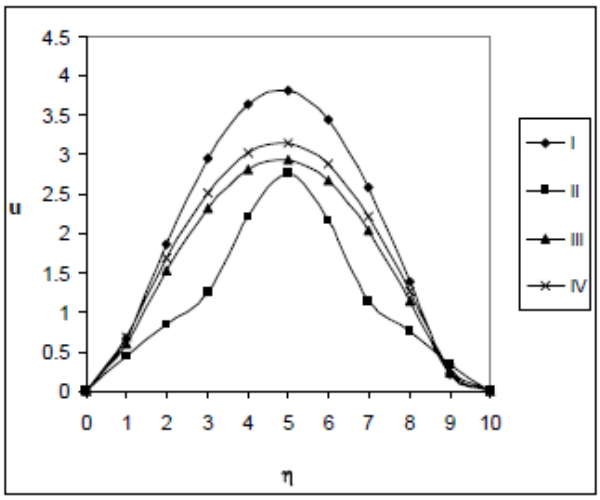

Fig. 4 : Variation of u with β

	I	II	III	IV
β	0.3	0.5	0.7	0.9

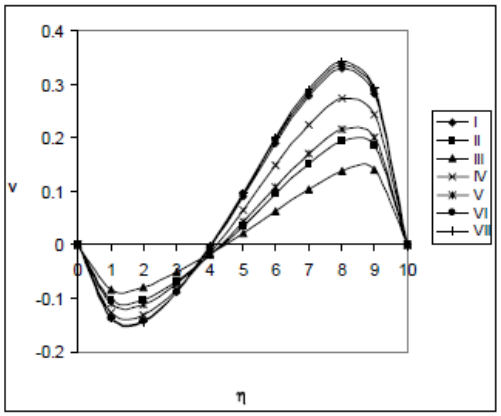

Fig. 5 : Variation of v with D^{-1}, M, m

	I	II	III	IV	V	VI	VII
D^{-1}	10^2	$2x10^2$	$3x10^2$	10^2	10^2	10^2	10^2
M	2	2	2	4	6	2	2
m	0.5	0.5	0.5	0.5	0.5	1.5	2.5

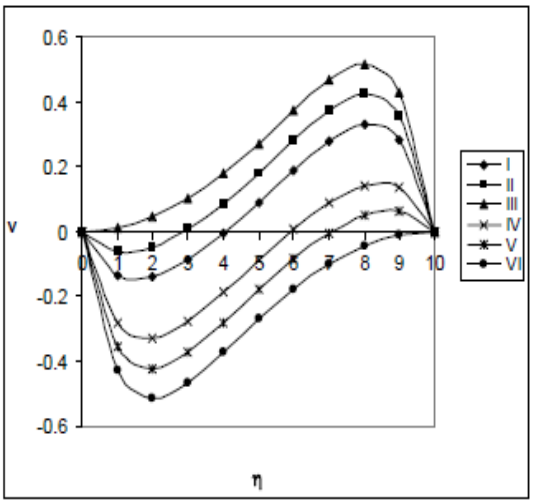

Fig. 6 : Variation of v with α

	I	II	III	IV	V	VI
α	2	4	6	-2	-4	-6

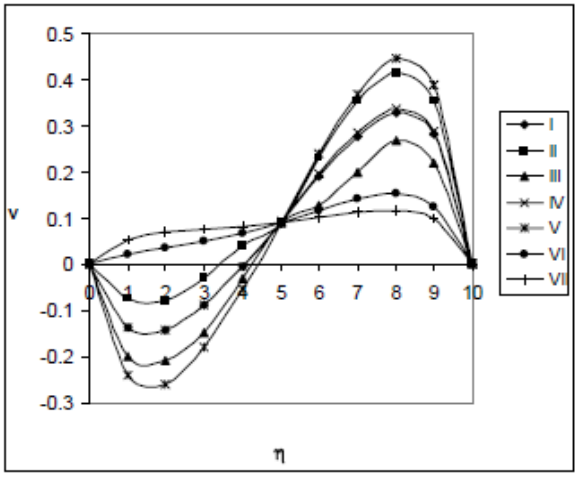

Fig. 7 : Variation of v with Sc, N

	I	II	III	IV	V	VI	VII
Sc	0.24	0.6	1.3	2.01	1.3	1.3	1.3
N	1	1	1	1	2	-0.5	-0.8

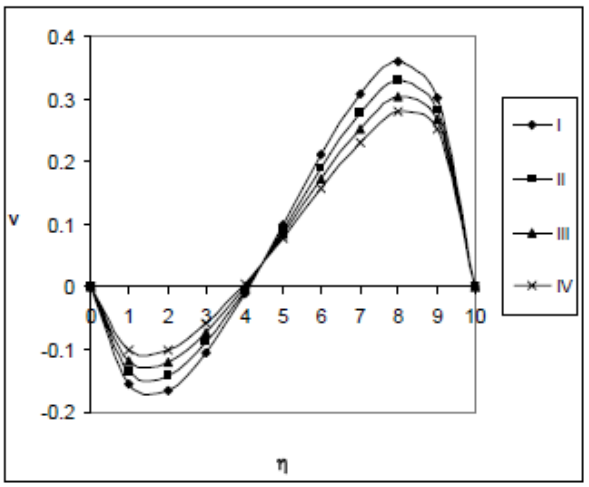

Fig. 8 : Variation of v with β

	I	II	III	IV
β	0.3	0.5	0.7	0.9

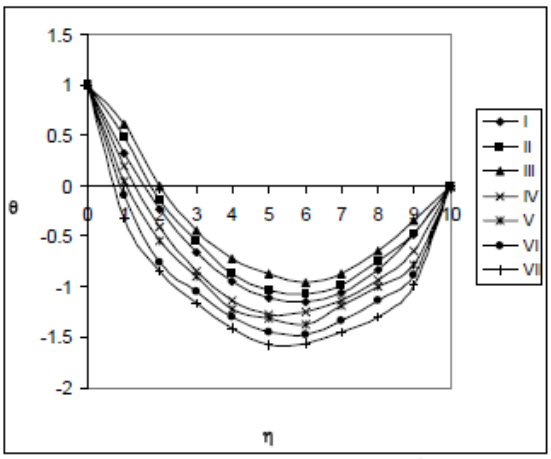

Fig. 9 : Variation of θ with D^{-1}, M, m

	I	II	III	IV	V	VI	VII
D^{-1}	10^2	$2x10^2$	$3x10^2$	10^2	10^2	10^2	10^2
M	2	2	2	4	6	2	2
m	0.5	0.5	0.5	0.5	0.5	1.5	2.5

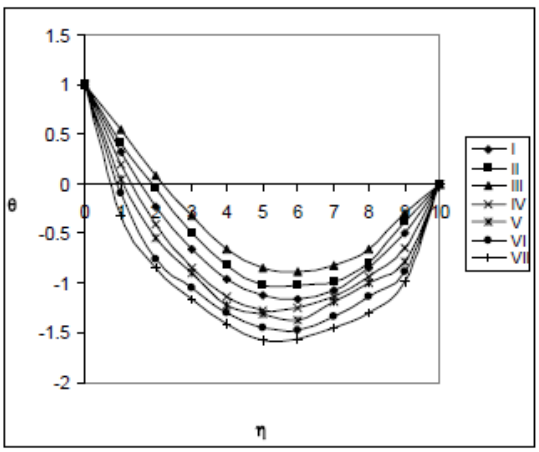

Fig. 10 : Variation of θ with α

	I	II	III	IV	V	VI	VII
Sc	0.24	0.6	1.3	2.01	1.3	1.3	1.3
N	1	1	1	1	2	-0.5	-0.8

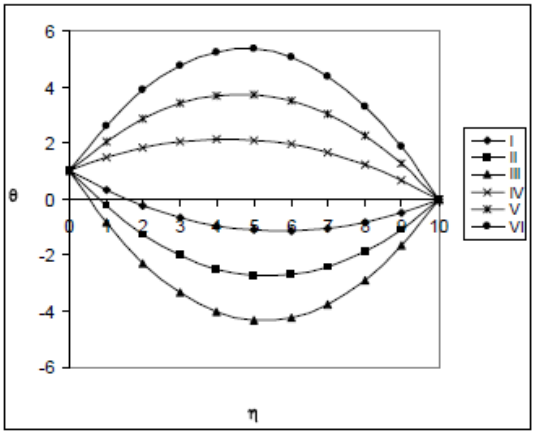

Fig. 11 : Variation of θ with Sc, N

	I	II	III	IV	V	VI
α	2	4	6	-2	-4	-6

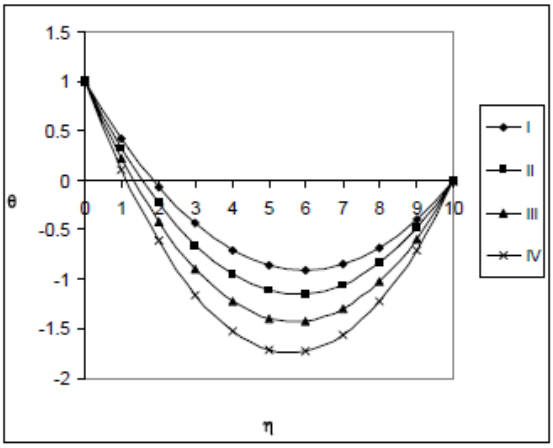

Fig. 12 : Variation of θ with β

	I	II	III	IV
β	0.3	0.5	0.7	0.9

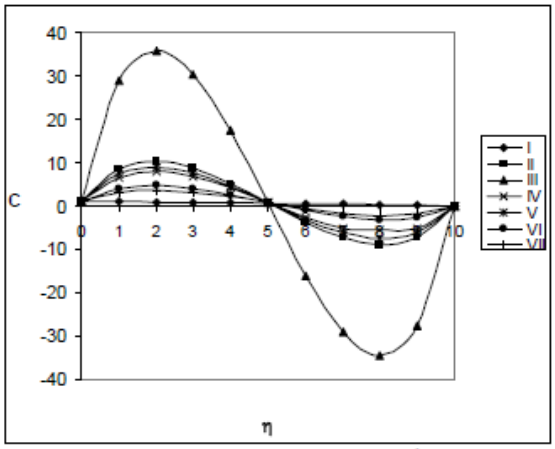

Fig. 13 : Variation of C with D^{-1}, M, m

	I	II	III	IV	V	VI	VII
D^{-1}	10^2	$2x10^2$	$3x10^2$	10^2	10^2	10^2	10^2
M	2	2	2	4	6	2	2
m	0.5	0.5	0.5	0.5	0.5	1.5	2.5

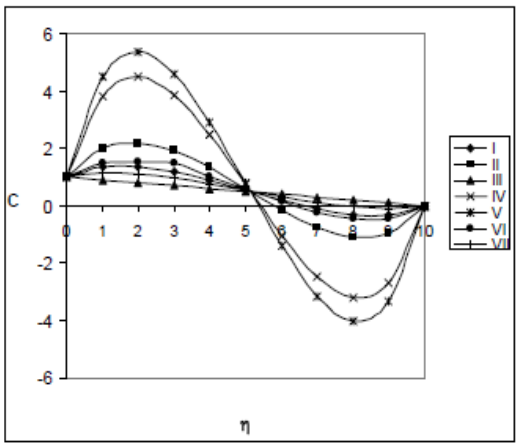

Fig. 14 : Variation of C with α

	I	II	III	IV	V	VI
α	2	4	6	-2	-4	-6

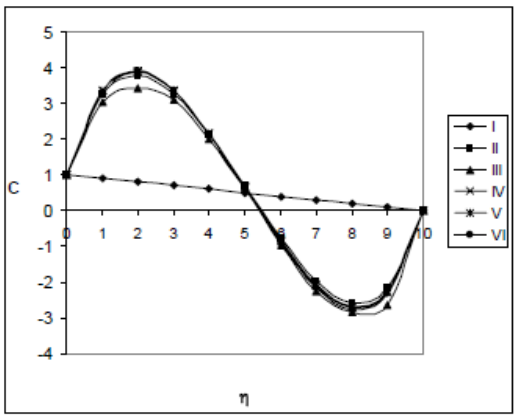

Fig. 15 : Variation of C with Sc, N

	I	II	III	IV	V	VI	VII
Sc	0.24	0.6	1.3	2.01	1.3	1.3	1.3
N	1	1	1	1	2	-0.5	-0.8

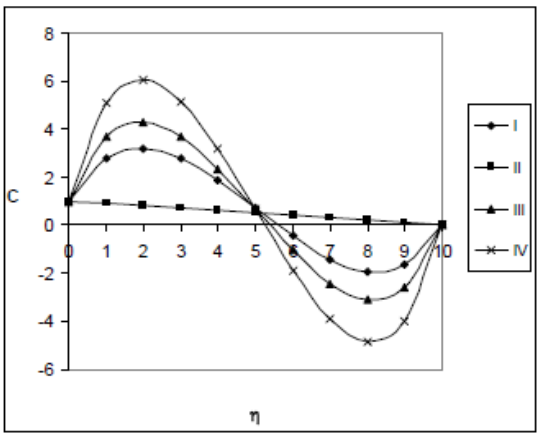

Fig. 16 : Variation of C with β

	I	II	III	IV
β	0.3	0.5	0.7	0.9

Tables:

Table-1
Average Nusselt Number (Nu) at η = +1

G	I	II	III	IV	V	VI	VII	VIII
5	0.1776	0.1484	0.1396	0.1347	0.1411	0.1363	0.1488	0.1495
10	0.2035	0.1640	0.1512	0.1435	0.1534	0.1462	0.1646	0.1655
-5	0.1260	0.1175	0.1166	0.1172	0.1167	0.1168	0.1176	0.1177
-10	0.1003	0.1022	0.1053	0.1085	0.1046	0.1072	0.1021	0.1020
D^{-1}	1	2	3	5	2	2	2	2
M	2	2	2	2	4	6	2	2
m	0.5	0.5	0.5	0.5	0.5	0.5	1.5	2.5

Table-2
Average Nusselt Number (Nu) at η = +1

G	I	II	III	IV	V	VI	VII
5	0.1484	0.1484	0.1484	0.1484	0.1414	0.1369	0.1347
10	0.1640	0.1640	0.1640	0.1640	0.1538	0.1471	0.1436
-5	0.1175	0.1175	0.1175	0.1175	0.1167	0.1168	0.1171
-10	0.1022	0.1022	0.1022	0.1022	0.1045	0.1068	0.1085
Sc	0.24	0.6	1.3	2.0	1.3	1.3	1.3
λ	0.25	0.25	0.25	0.25	0.5	0.75	1

Table-3
Average Nusselt Number (Nu) at η = +1

G	I	II	III	IV	V	VI	VII	VIII	IX
5	0.1484	0.1059	0.9376	-0.3688	-0.1456	-0.1093	0.1562	0.1368	0.1345
10	0.1640	0.1197	0.1067	-0.3606	-0.1348	-0.9729	0.1797	0.1407	0.1360
-5	0.1175	0.7846	0.6796	-0.3856	-0.1673	-0.1333	0.1099	0.1291	0.1314
-10	0.1022	0.6480	0.5511	-0.3943	-0.1783	-0.1454	0.8704	0.1252	0.1298
α	2	4	6	-2	-4	-6	2	2	2
N	1	1	1	1	1	1	2	-0.5	-0.8

Table-4
Average Nusselt Number (Nu) at η = +1

G	I	II	III	IV	V	VI
5	0.1742	0.1484	0.1256	0.1063	0.1484	0.1484
10	0.1878	0.1640	0.1411	0.1208	0.1640	0.1640
-5	0.1473	0.1175	0.9498	0.7759	0.1175	0.1175
-10	0.1339	0.1022	0.7983	0.6344	0.1022	0.1022
β	0.3	0.5	0.7	0.9	0.5	0.5
R	35	35	35	35	70	140

Table-5

Average Nusselt Number (Nu) at η = -1

G	I	II	III	IV	V	VI	VII	VIII
5	0.8381	0.1915	0.2183	0.2708	0.2123	0.2412	0.1905	0.1890
10	0.9467	0.2128	0.2546	0.3558	0.2441	0.2977	0.2115	0.2094
-5	0.6212	0.1496	0.1469	0.1035	0.1496	0.1301	0.1492	0.1486
-10	0.5129	0.1289	0.1117	0.2120	0.1188	0.7535	0.1289	0.1287
D^{-1}	1	2	3	5	2	2	2	2
M	2	2	2	2	4	6	2	2
m	0.5	0.5	0.5	0.5	0.5	0.5	1.5	2.5

Table-6

Average Nusselt Number (Nu) at η = -1

G	I	II	III	IV	V	VI	VII
5	0.1915	0.1915	0.1915	0.1915	0.2113	0.2352	0.2693
10	0.2128	0.2128	0.2128	0.2128	0.2424	0.2860	0.3529
-5	0.1496	0.1496	0.1496	0.1496	0.1500	0.1351	0.1049
-10	0.1289	0.1289	0.1289	0.1289	0.1198	0.8580	0.2397
Sc	0.24	0.6	1.3	2.0	1.3	1.3	1.3
λ	0.25	0.25	0.25	0.25	0.5	0.75	1

Table-7

Average Nusselt Number (Nu) at η = -1

G	I	II	III	IV	V	VI	VII	VIII	IX
5	0.1915	0.7938	0.3577	-0.1838	-0.7178	-0.2503	0.2022	0.1757	0.1726
10	0.2128	0.9199	0.4497	-0.1950	-0.7555	-0.2613	0.2343	0.1810	0.1747
-5	0.1496	0.5568	0.1746	-0.1611	-0.6417	-0.2281	0.1393	0.1652	0.1684
-10	0.1289	0.4368	0.8341	-0.1496	-0.6034	-0.2169	0.1085	0.1600	0.1663
α	2	4	6	-2	-4	-6	2	2	2
N	1	1	1	1	1	1	2	-0.5	-0.8

Table-8

Average Nusselt Number (Nu) at η = -1

G	I	II	III	IV	V	VI
5	0.2370	0.1915	0.1620	0.1419	0.1915	0.1915
10	0.2508	0.2128	0.1896	0.1754	0.2128	0.2128
-5	0.2097	0.1496	0.1075	0.7629	0.1496	0.1496
-10	0.1961	0.1289	0.8074	0.4402	0.1289	0.1289
β	0.3	0.5	0.7	0.9	0.5	0.5
R	35	35	35	35	70	140

Table-9

Sherwood number (Sh) at η = +1

G	I	II	III	IV	V	VI	VII	VIII
5	-0.8884	-0.7462	-0.6936	-0.6142	-0.7055	-0.6539	-0.7480	-0.7508
10	-0.8701	-0.8309	-0.8189	-0.7700	-0.8227	-0.7993	-0.8312	-0.8317
-5	-0.7920	-0.1311	-0.1835	-0.3103	-0.1693	-0.2404	-0.1279	-0.1278
-10	-0.8178	-0.1088	-0.1289	-0.1543	-0.1242	-0.1435	-0.1082	-0.1073
D^{-1}	1	2	3	5	2	2	2	2
M	2	2	2	2	4	6	2	2
m	0.5	0.5	0.5	0.5	0.5	0.5	1.5	2.5

Table-10

Sherwood number (Sh) at $\eta = +1$

G	I	II	III	IV	V	VI	VII
5	-0.3324	-0.5604	-0.7462	0.8298	-0.7075	-0.6634	-0.6160
10	-0.4898	-0.7008	-0.8309	-0.8806	-0.8233	-0.8050	-0.7714
-5	0.9209	-0.3696	-0.1311	-0.1096	-0.1670	-0.2254	-0.3069
-10	-0.5668	-0.1472	-0.1088	-0.1008	-0.1234	-0.1403	-0.1539
Sc	0.24	0.6	1.3	2.0	1.3	1.3	1.3
λ	0.25	0.25	0.25	0.25	0.5	0.75	1

Table-11

Sherwood number (Sh) at $\eta = +1$

G	I	II	III	IV	V	VI	VII	VIII	IX
5	-0.7462	-0.8276	-0.9159	-0.6021	-0.5388	-0.4808	-0.7990	-0.9919	-0.3314
10	-0.8309	-0.8812	-0.9366	-0.7446	-0.7082	-0.6761	-0.8636	-0.6318	-0.4539
-5	-0.1311	-0.1158	-0.1023	-0.1677	-0.1897	-0.2145	-0.1153	-0.2941	0.2499
-10	-0.1088	-0.1031	-0.9801	-0.1225	-0.1305	-0.1394	-0.1031	-0.2333	0.1296
α	2	4	6	-2	-4	-6	2	2	2
N	1	1	1	1	1	1	2	-0.5	-0.8

Table-12

Sherwood number (Sh) at $\eta = +1$

G	I	II	III	IV	V	VI
5	-0.7073	-0.7462	-0.7424	-0.7236	-0.8823	-0.9564
10	-0.8235	-0.8309	-0.8103	-0.7810	-0.9089	-0.9471
-5	-0.1784	-0.1311	-0.1144	-0.1043	-0.1007	-0.9179
-10	-0.1262	-0.1088	-0.9984	-0.9327	-0.9699	-0.9274
β	0.3	0.5	0.7	0.9	0.5	0.5
R	35	35	35	35	70	140

Table-13

Sherwood number (Sh) at $\eta = -1$

G	I	II	III	IV	V	VI	VII	VIII
5	0.7634	0.1053	0.1238	0.1510	0.1194	0.1379	0.1047	0.1039
10	0.8602	0.1093	0.1262	0.1524	0.1222	0.1397	0.1088	0.1080
-5	0.1095	0.1202	0.1335	0.1570	0.1301	0.1454	0.1199	0.1193
-10	0.1028	0.1170	0.1314	0.1557	0.1278	0.1438	0.1166	0.1160
D^{-1}	1	2	3	5	2	2	2	2
M	2	2	2	2	4	6	2	2
m	0.5	0.5	0.5	0.5	0.5	0.5	1.5	2.5

Table-14
Sherwood number (Sh) at $\eta = -1$

G	I	II	III	IV	V	VI	VII
5	0.1035	0.1049	0.1053	0.1055	0.1187	0.1346	0.1505
10	0.1071	0.1087	0.1093	0.1095	0.1215	0.1365	0.1518
-5	0.1193	0.1200	0.1202	0.1203	0.1296	0.1425	0.1565
-10	0.1164	0.1168	0.1170	0.1170	0.1272	0.1408	0.1552
Sc	0.24	0.6	1.3	2.0	1.3	1.3	1.3
λ	0.25	0.25	0.25	0.25	0.5	0.75	1

Table-15
Sherwood number (Sh) at $\eta = -1$

G	I	II	III	IV	V	VI	VII	VIII	IX
5	0.1053	0.9555	0.8451	0.1215	0.1281	0.1338	0.1082	0.7278	-0.9013
10	0.1093	0.1041	0.9819	0.1174	0.1204	0.1228	0.1107	0.9525	0.5571
-5	0.1202	0.1264	0.1318	0.1052	0.9609	0.8589	0.1181	0.1361	0.1567
-10	0.1170	0.1199	0.1222	0.1092	0.1042	0.9848	0.1159	0.1256	0.1392
α	2	4	6	-2	-4	-6	2	2	2
N	1	1	1	1	1	1	2	-0.5	-0.8

Table-16
Sherwood number (Sh) at $\eta = -1$

G	I	II	III	IV	V	VI
5	0.1078	0.1053	0.1032	0.1014	0.1057	0.1057
10	0.1123	0.1093	0.1068	0.1046	0.1097	0.1097
-5	0.1247	0.1202	0.1167	0.1138	0.1204	0.1204
-10	0.1210	0.1170	0.1137	0.1110	0.1171	0.1171
β	0.3	0.5	0.7	0.9	0.5	0.5
R	35	35	35	35	70	140

